Comparison of 1-D, 2-D and 3-D Printer Calibration Algorithms with Printer Drift

Prudhvi K. Gurram and Sohail A. Dianat, Department of Electrical Engineering, Rochester Institute of Technology, Rochester, New York, USA; Lalit K. Mestha, Wilson Center for Research and Technology, Xerox Corporation, Webster, New York, USA; Raja Bala, Imaging Services and Technology Center, Xerox Corporation, Webster, New York, USA

Abstract

For consistent color reproduction, a digital printer must operate in a stable mode. However, due to uncertainties such as changes in humidity and temperature, color printers drift over time. Calibration is an approach that can be used to bring back the printer to its initial state from a drifted state. Different algorithms are used to calibrate printers. Among them are one-dimensional gray balance[1], one-dimensional channelwise linearization[1], two-dimensional calibration[1], and three-dimensional calibration[2]. In this paper, we benchmark the performance of different calibration algorithms in stabilization of digital color printers subject to printer drift. The figure of merit used for comparison is the improvement in CIELAB ΔE *between the output of calibrated machine and the output of the machine in a drifted mode for the same input. We also examine the optimum number of color patches needed to be measured for calibrating the machine with different calibration algorithms. The optimum number of patches is selected using dynamic optimization algorithm[3]. Simulation results are presented using real printer data.*

Introduction

Any imaging system can be seen as a mapping from a device-specific color space to a device-independent color space. The mapping is a Look up Table (LUT) from one space to another. The color printer in specific is a mapping from device-specific color space (e.g., *CMY)* to device-independent color space (e.g., *L*a*b**). *L*a*b** created by CIE defines the perceptually uniform color space that is correlated with the visual appearance of colors. *CMY* and *CMYK* color spaces are used in four-color printing process as its primaries. *CMYK* color space is a variation of the *CMY* model. It adds extra black as primary by removing black component in *CMY*. For simplicity, throughout this paper, we use the *CMY* primaries and ignore the black separation. One of the most crucial challenges facing today's digital printer manufacturers is to design printers that accurately and consistently reproduce the customer colors in images[2]. Printers are calibrated with inverse maps more frequently to meet those challenges. Usually, the mapping from the input color space to the output color space is highly non-linear and drifts over time. This is further enhanced by the variants in the physical properties of the system due to temperature, moisture content, brightness, and media. As a result, printers reproduce inaccurate and inconsistent colors. So the printers need to be recalibrated quite frequently. After calibration, the color-separated image is converted into halftones and delivered to the print engine for physical reproduction of the prints. The process of printing is shown schematically in Fig. 1.

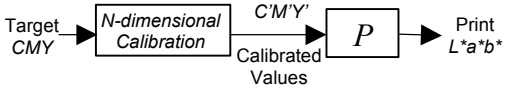

Figure 1. The Process of Digital Printing

This paper first discusses various printer calibration approaches. We compare the performance of these approaches based on the simulations performed using practical printer data. We create a numerical drift model using measured data. The method used to develop the printer drift model is explained. We show printer calibration results in the presence of drift using the drift model. Furthermore, a novel measurement reduction algorithm is used to reduce time sampling of printer drift. The effect of reduced measurements on each calibration approach is discussed in the final section.

One-Dimensional Calibration

In this method, correction is made along each independent channel of the printer. This correction in each channel is called Tone Response Curve (TRC). So, a *CMY* printer is calibrated using three TRCs, one for each color separation.

Channelwise Linearization to ΔE from Paper

In this method the TRC for each channel is built by linearizing the Δ*E* from paper. This is to make the printer emulate an ideal printer which has the characteristic of linearized Δ*E* from paper. Δ*E* from paper is the Euclidean norm between target color and the medium paper white1 in the device-independent color space (L*a*b*). To build the TRC for a single channel, input color patches are generated by increasing that particular channel (d) from 0 to 255 while the other two channels are set at 0. Δ*E* difference from medium white is found for the channel. A straight line is drawn from the Δ*E* of the medium (d=0) to the Δ*E* of the maximum channel input value (d=255). And the inverse of the Δ*E* from paper curve with respect to the straight line is found. An example of this process is shown in Fig. 2.

Gray-Balanced Calibration

Gray-balance calibration is also a one-dimensional calibration technique. Gray is a color lacking hue (also called achromatic color) and is generated by mixing C, M, Y primary colors[4]. Gray balance involves finding the proper percentage of combinations of primaries that produce different shades of gray. The one-dimensional channelwise linearization assumes that the non-linearity in the printer transformation in one channel is

independent of the non-linearity in another channel. On the other hand, the gray-balance is preferred over channelwise linearization because it takes the first order dependence among 3 channels of the printer into account. One more reason for preferring gray-balance over channelwise linearization is that human visual system is more sensitive to the color differences near the gray axis.[1] Any color on the neutral axis i.e. $C=M=Y=d$ transforms ideally to $L=L^*$, $a^*=0$, $b^*=0$. For an ideal printer that can produce shades of gray between L*=100 and L*=0, the ideal $L^*a^*b^*$ values corresponding to the gray patches $C=M=Y=d$ are found using Eq. (1) where d goes from 0 to 255.

$$L^* = 100 - (d \times 100) / 255,\ a^* = 0,\ b^* = 0 \quad (1)$$

(Note that Equation (1) is just an illustration; in reality, printers can only produce shades of gray down to some minimum L*.) The ideal $L^*a^*b^*$ values are passed through the inverse printer mapping LUT as shown in Fig. 3. The inverse printer mapping is built using Iterative Clustered Interpolation[2] (ICI) algorithm. C'M'Y' values (see in Fig. 3) are the TRCs (which are smoothened to remove glitches using algorithms shown in Reference 4) for the three channels of the printer. The output L*a*b* values and the ideal L*a*b* values satisfy Eq. (2)

$$\Delta E = \| L^*a^*b^*_{ideal} - L^*a^*b^*_{out} \|_2 \approx 0 \quad (2)$$

In one-dimensional calibration, the corrected value for any *CMY* patch is obtained by passing it through the TRC LUT as shown in Fig. 4.

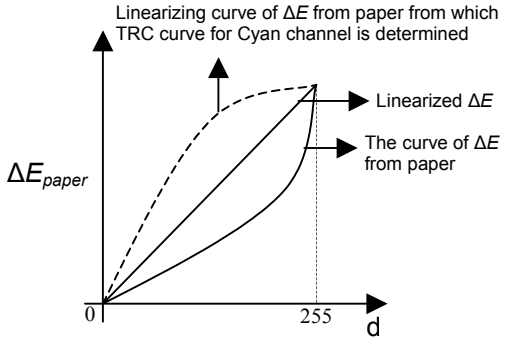

Figure 2. Sample curve of ΔE from paper

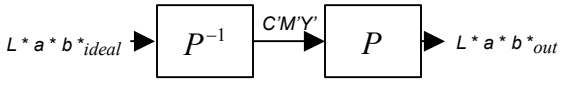

Figure 3. Three Channel Gray-balance

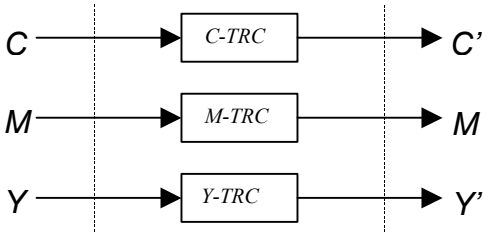

Figure 4. One-dimensional TRC model

Two-Dimensional Calibration

Two-dimensional calibration[1] technique involves calibration of *CMY* patches using three two-dimensional LUTs, one for each channel. The inputs to these LUTs are functions of the input *CMY* values. For instance the inputs to the LUT, which determines the transformation for the Cyan channel, are C and $M+Y$. Similarly for Magenta channel, the inputs are M and $C+Y$ and for Yellow channel, the inputs are Y and $C+M$. The corrected *CMY* values are given by Eqs. (3), (4) and (5).

$$C' = f_1(C, M+Y) \quad (3)$$

$$M' = f_2(M, C+Y) \quad (4)$$

$$Y' = f_3(Y, C+M) \quad (5)$$

The functions f_1, f_2, and f_3 are implemented in full resolution 2-D LUTs that require no interpolation.[1] Fig. 5 shows the two-dimensional LUT for each channel and the five axes along which one-dimensional calibration is used to fill the LUT. In a simple implementation, axes 1, 2, 4 and 5 are calibrated using channelwise calibration while axis 3 is calibrated using gray-balanced calibration. The intermediate regions of the 2D LUT are then filled with 2-D sequential linear interpolation[5] among these 5 axes. The corrected value for a *CMY* patch is obtained as shown in Fig. 6. Since the 2D LUTs are pre-filled for all possible input combinations, the LUT processing involves only indexing and lookup operations.

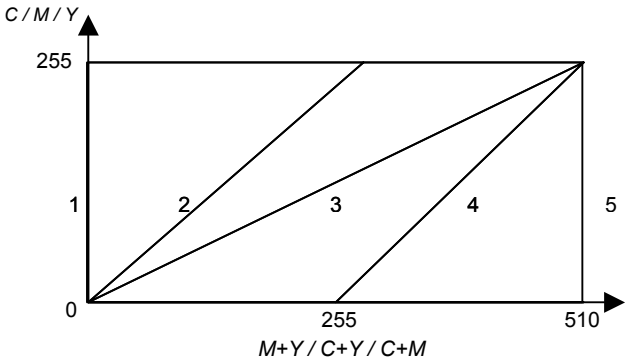

Figure 5. Two-dimensional LUT for each channel

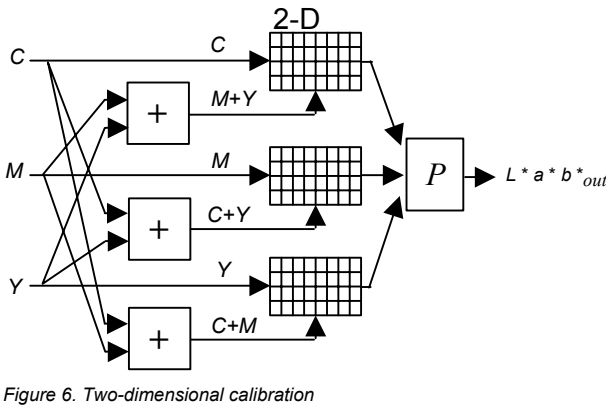

Figure 6. Two-dimensional calibration

Three-Dimensional Calibration

Three-dimensional calibration technique provides the best results because it is nothing but the inverse printer mapping for every color in the node preceding the forward printer mapping. The inverse printer map is developed from the forward printer map using ICI algorithm. The iteratively clustered interpolation is a gradient-based optimization method to compute an accurate structured inverse table from irregularly sampled color data with initial points for optimization obtained by the clustering technique. In three-dimensional calibration, the requested color patch to be printed is obtained in the device-independent color space i.e. *L*a*b** color space and then passed through the inverse printer transformation to obtain the calibrated *C'M'Y'* values as shown in Fig. 7. If the requested color data is not present in any of the maps, the output is obtained by using trilinear interpolation. The *C'M'Y'* values are passed through the printer to print the color patch on the paper.

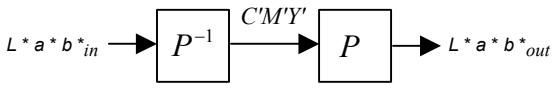

Figure 7. Three-dimensional Calibration

Printer Drift Model

In this section it is explained how a drifted printer mapping *P(t)* is built from the initial forward printer mapping $P(t_0)$. It is easy to build a printer drift model if the measurements for all the patches in the input color space of the printer LUT are available at any instant of time. Such a printer drift model is valid for the duration of the measurement set. But here an attempt is made to build the drift model with very few measurements made by printing the patches along the gray axis or the neutral.

Available Drift Data

The drift measurements for 33 patches along the gray axis are available for 1200 different time instants. The drift measurements for these 33 patches are used to determine the drift model of the printer at any time instant within the measurement time period, and for many colors slightly away from the neutral axis.

Drift Data Boundary Conditions

Each available patch on the neutral axis is projected on all the faces and edges of the structured cubic input color space as shown in Fig. 8. Each patch on the neutral generates 18 projected points (or patches). As the drift data for these patches is not available, we assumed that there is no drift in all of these boundary patches (which is an approximation). The 8 corner points of the structured *CMY* color space are also assumed to have no drift. The output *L*a*b** values for all these patches are obtained by using trilinear interpolation on the forward printer mapping LUT at time t_0.

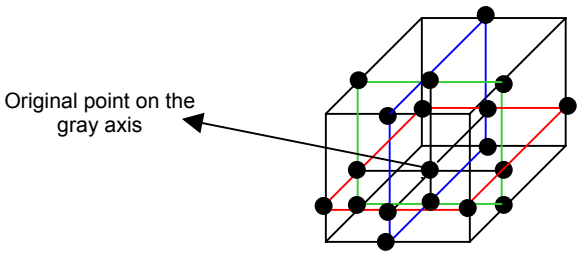

Figure 8. Projection of a gray point on all the 6 faces and 12 edges of the structured CMY color space

Printer Model at a Time Instant 't'

With the help of the available and boundary drift data, the drift values for the remaining patches in the structured *CMY* color space are found. As the data is not present on a regular grid, three-dimensional sequential linear interpolation[5] technique is used to determine the drift values for the rest of the patches. So, finally a printer drift model is obtained and the time varying printer LUT is as shown schematically in Fig. 9. We remark that while this drift model is simplistic, it does exhibit the important characteristic that the drift mechanism varies as a function of location in color space.

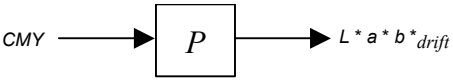

Figure 9. Printer drift model at time instant 't'

Calibration with Reduced Measurements

To calibrate a digital printer with reduced patch measurements, first the n-dimensional (*n=1, 2,* and *3*) calibration LUTs for the printer at 't_0' are determined. These LUTs are down-sampled using Dynamic Optimization[3] (DO) algorithm. This algorithm finds the reduced set of optimal points which best represents the LUT i.e. when the LUT is re-built (up-sampled) from the reduced set using n-dimensional linear interpolation, the mean square error (MSE) between the original LUT and re-built LUT would be minimum. The same reduced set of nodes in *CMY* space is used to build the re-calibration LUTs at any instant '*t*'.

Experiment

The experiments are performed initially at t_0 on two sets of data to compare different methods of printer calibration. The accuracy of the methods when re-calibration is performed at a later time, *t* are also compared. The effect of reduced patch measurements is also compared for different calibration algorithms on input data from one of the two data sets (see next section).

Experimental Data

The first set of data, Set 1, contains 30 patches on each of the axes 1, 2, 4, and 5 in each of the three two-dimensional LUTs shown in Fig. 5 and 30 patches on the neutral. This brings the total number of patches to 390 out of which 12 of them repeat. So, Set 1 contains 378 color patches on the boundary of the printer gamut and neutral axis. The second set of data, Set 2, contains 180 in-gamut color patches which include 24 patches on the neutral. This set is used to determine the effect of calibration inside the gamut.

These sets of data are used as target *CMY* values in Fig. 10 and Fig. 11.

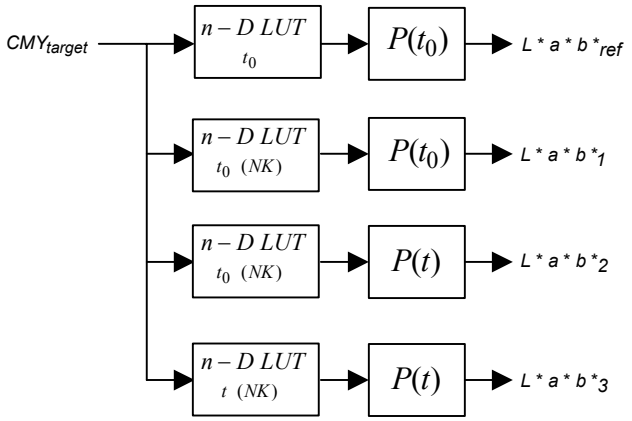

Figure 10. Simulation performed for 1-D and 2-D calibration techniques (NK = 3, 5, 10, 20, 256)

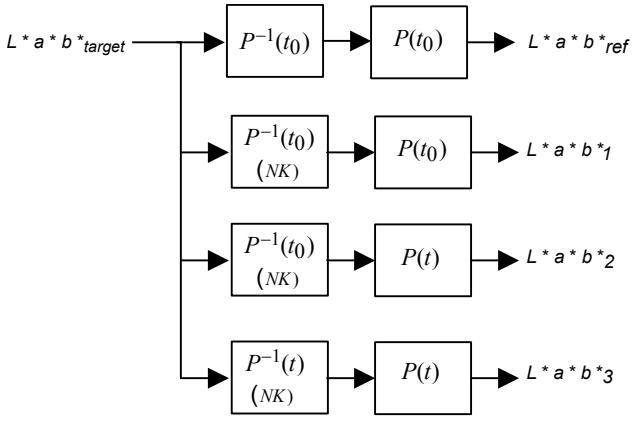

Figure 11. Simulation performed for 3-D Calibration technique (NK =3^3, 4^3, 5^3, 6^3, 13^3)

Experiments Performed

The experiments performed using one-dimensional and two-dimensional calibration techniques vary a little from those performed using three-dimensional calibration technique as the inputs in the two cases are in different color spaces. The simulations performed for one-dimensional and two-dimensional calibration techniques at different times of calibration and measurement of ΔE are as shown in Fig. 10. The simulations performed for three-dimensional calibration algorithms are as shown in Fig. 11. The figure of merit ΔE is calculated using Eq. (6).

$$\Delta E = \|L^*a^*b^*_i - L^*a^*b^*_{ref}\|,\ i = 1, 2, 3 \qquad (6)$$

Where $L^*a^*b^*_{ref}$ is the $L^*a^*b^*$ values of Set 1 test patches after calibrating the printer at time t_0 and $L^*a^*b^*_i$, i=1, 2, 3 are $L^*a^*b^*$ values of Set 1 test patches at different times using different calibration techniques as indicated in Fig. 10 and 11. In two-dimensional calibration, the TRCs along each of the axes are down-sampled. In Fig. 10, NK = 256 represents the original case without any down-sampling. In that case $L^*a^*b^*_1$ is the same as $L^*a^*b^*_{ref}$.

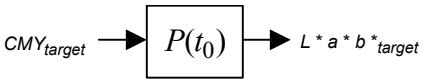

Figure 12. Generation of target data for 3-D Calibration

In three-dimensional calibration, the target data in $L^*a^*b^*$ space is obtained from the target data in *CMY* space as shown in Fig. 12. In Fig. 11, NK = 13^3 represents the case without down-sampling as the gamut of the printer is being sampled with 13^3 points.

Results and Summary

The forward printer mapping at t_0 is available and the drift model of the printer at t = t_0+*300* is determined from the available measurements. The experiments are performed on this drifted printer mapping. The drift statistics are as shown in table 1. As some of the points in the gamuts are assumed to have no drift, the drift statistics are small.

Table 1: Drift Statistics

ΔE	Mean	Maximum	95 Percentile
Statistics	3.114	10.65	6.56

The graph in Fig. 13 shows the improvement in ΔE between the output of the calibrated machine and the output of the drifted machine for input data from Set 1. The graph in Fig. 14 shows the same for input data from Set 2. ΔE measured at t_0 in each approach is zero because the output obtained in that simulation (when there is no down-sampling) is taken as the reference for that approach (since ΔE is calculated with respect to $L^*a^*b^*_{ref}$ as shown in Fig. 10 and 11). At t_0 the ΔE with respect to $L^*a^*b^*_{target}$ ($L^*a^*b^*_{target}$ to $L^*a^*b^*_{ref}$ as shown in Fig.11) for a three dimensional calibration has a mean of 1.435 which is introduced by the three dimensional calibration LUT. It can be seen from both the graphs that ΔE improves for two-dimensional calibration and three-dimensional calibration. Also two-dimensional calibration does a better job than three-dimensional calibration along the boundary of the printer gamut (Set 1) while it's the contrary inside the gamut (Set 2). This difference is due to the linear interpolation in the inverse and forward printer maps. The one-dimensional channelwise linearization algorithm shows no improvement in ΔE because the TRCs in this algorithm depend on the drift along the boundary of the gamut since in our drift model we assumed no drift for boundary colors. So the TRCs remain the same even during re-calibration. As a result there is no improvement. The one-dimensional gray-balanced calibration algorithm actually has deterioration effect on ΔE. The reason for this is that the printer drift model is constructed with the assumption that there is drift along the neutral axis and this drift is linearly approaching zero as we move toward the gamut boundary. The TRCs at time t which are constructed based on the drift along the neutral axis expect similar drift throughout the printer gamut. However the drift model used has little or no drift for colors off the neutral axis and near the gamut boundary. The graphs in Fig. 15-18 show the effect of down-sampling the number of patch measurements for calibrating

the printer. Here the input is taken from Set 2 to show the effects inside the gamut. It can be seen from the graphs that as the number of patch measurements decrease, the output also gets worse as a result of which ΔE from the reference (which is the output of the printer with all the measurements) increases in all the algorithms. For one-dimensional calibration techniques, there is not much change in ΔE for NK=5, 10, 20, 256 measurements. So it can be concluded that 5 patch measurements are enough for calibration of the printer with the given drift model. For two-dimensional calibration technique, there is not much change in ΔE for NK=5, 10, 20, 256 measurements on each axis of the LUT. And for three-dimensional calibration, there is decrease in ΔE all through except for the case in which the calibration LUT is built for the printer at t_0 and ΔE is measured at t.

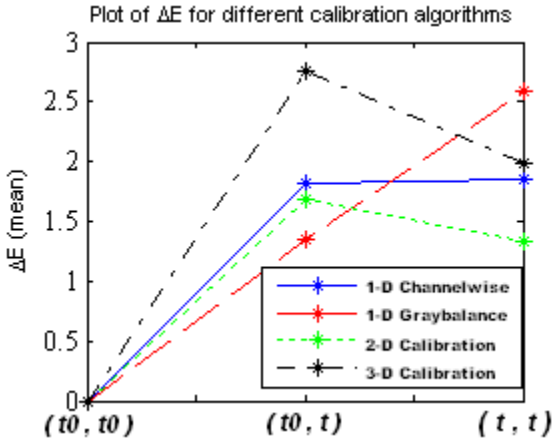

Figure 13. Plot of ΔE (mean) at different instants of calibration and measurement for input from Set 1

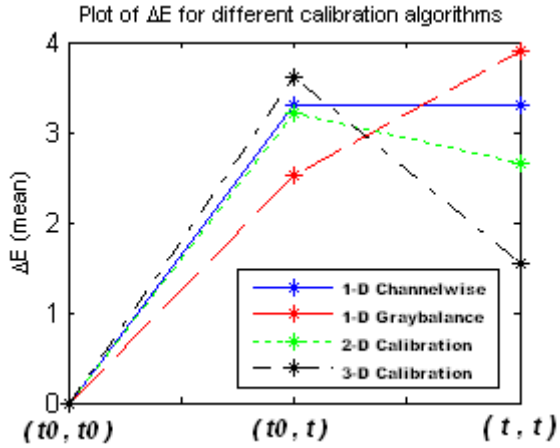

Figure 14. Plot of ΔE (mean) at different instants of calibration and measurement for input from Set 2

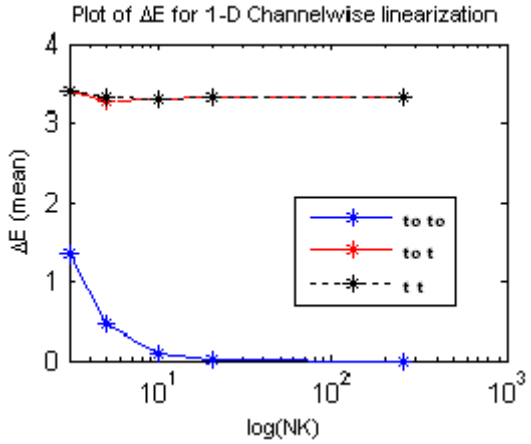

Figure 15. Plot of ΔE (mean) for different no. of patch measurements at different times of calibration and measurement for 1-D Channelwise linearization

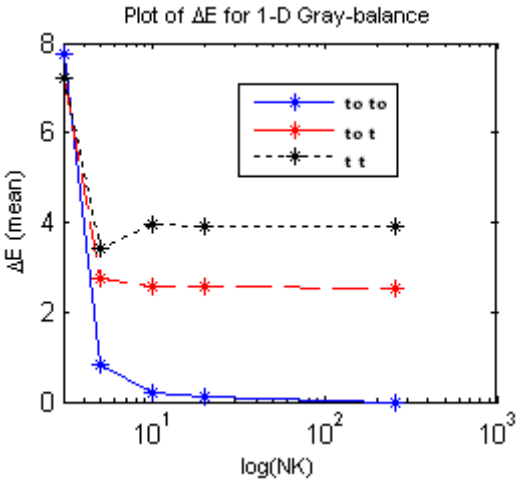

Figure 16. Plot of ΔE (mean) for different no. of patch measurements at different times of calibration and measurement for 1-D Gray-balance

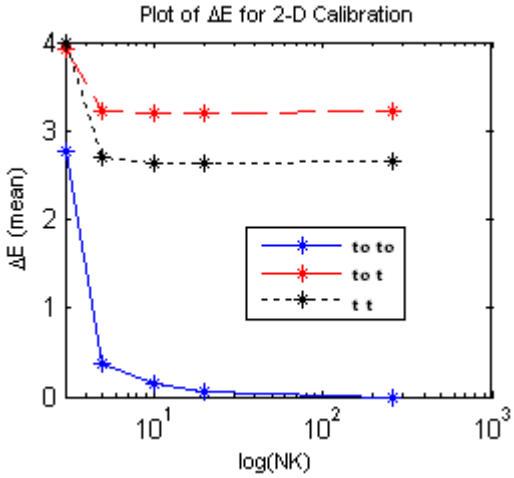

Figure 17. Plot of ΔE (mean) for different no. of patch measurements at different times of calibration and measurement for 2-D Calibration

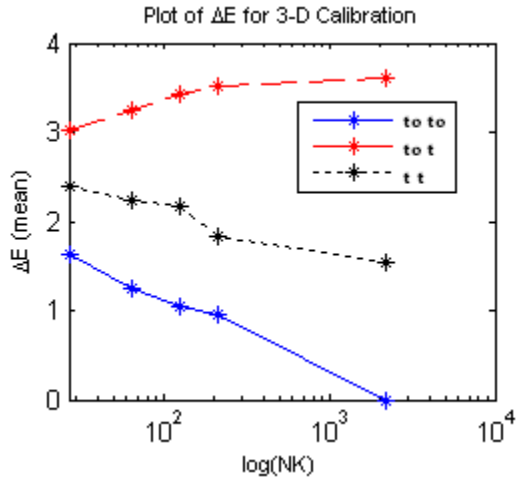

Figure 18. Plot of ΔE (mean) for different no. of patch measurements at different times of calibration and measurement for 3-D Calibration

References

1. R. Bala, G. Sharma, V. Monga, J. P. VandeCapelle, "Two-Dimensional Transforms for Device Color Correction and Calibration," submitted to IEEE Trans. on Image Processing, March 2004.
2. L. K. Mestha, Y. R. Wang, S. A. Dianat, and D. E. Viassalo, “Iterative clustering interpolation algorithm for geometrical interpolation of an irregularly spaced multidimensional color space,” in Proc. 2000 IS&T Conf. On Digital Printing Technologies (NIP16), Vol. 9, pp. 267-270 (2000).
3. S. A. Dianat and L.K. Mestha, “Dynamic Optimization Algorithm for Generating Inverse Printer Maps with Reduced Measurements”, Paper submitted to IEEE Conference on Decision & Control 2004, Dec 12-15 2005, Seville, Spain.
4. Lalit K. Mestha, R. Enrique Viturro, Yao Rong Wang, Sohail A. Dianat “Gray Balance Control Loops for Digital Color Printing Systems”, IS&T’s NIP21 Conference.
5. J. Z. Chang, “Sequential Linear Interpolation of Multidimensional Functions,” IEEE Trans. on Image Processing, vol. 6, pp. 1231-1245, September 1997.

Author Biographies

Prudhvi Gurram received his B.E in Electronics and Communication Engineering from the National Institute of Technology Karnataka, India (2003). Currently, he is working towards his M.S degree in Electrical Engineering at Rochester Institute of Technology. He is working on Printer Calibration for his M.S thesis.

Sohail A. Dianat received the B.S. degree from Arya-Mehr University, Tehran, Iran in 1973, and the M.S. and D.Sc. degrees from George Washington University in 1976 and 1981, respectively, all in electrical engineering. Professor Dianat has been with the Department of Electrical Engineering at RIT since 1981. Sohail is the author of numerous publications. He received the "best unclassified paper award" at the MILCOM '93. He is fellow member of SPIE and a member of IEEE.

L.K. Mestha, a Principal Scientist at Xerox, received his PhD from the University of Bath, England in 1985 and his BE in 1982, from the University of Mysore, India, all in EE. He has worked on sensing & control of printing systems since 1994. He holds 40 US Patents and has a total of 100 publications including patents & filings. Prior to joining Xerox, Mestha was at the SSC Laboratory in Dallas. He is a Senior Member of IEEE, a member of IS&T and teaches at RIT as an Adjunct Professor.

Raja Bala received the B.S. degree from the University of Texas at Arlington in 1987, and the M.S. and Ph.D. degrees from Purdue University in 1988 and 1992, respectively, all in Electrical Engineering. He is currently a Principal Scientist in the Xerox Innovation Group, working on color imaging algorithms for Xerox's color products. Raja is also an Adjunct Professor in the EE- Dept RIT. He holds over 30 patents and over 40 publications in the field of color imaging. He is a member of IS&T.